Mon. Not. R. Astron. Soc. **370,** 743–752 (2006) doi:10.1111/j.1365-2966.2006.10481.x

NGC 7419: a young open cluster with a number of very young intermediate mass pre-MS stars

Annapurni Subramaniam,[1⋆] Blesson Mathew,[1] Bhuwan Chandra Bhatt[2] and S. Ramya[1]

[1]*Indian Institute of Astrophysics, Bangalore 560034, India*
[2]*CREST Campus, Indian Institute of Astrophysics, PO Box 19, Hosakote, Bangalore 562114, India*

Accepted 2006 April 19. Received 2006 April 3; in original form 2006 February 10

ABSTRACT

We present a photometric and spectroscopic study of the young open cluster NGC 7419, which is known to host a large number of classical Be stars for reasons not well understood. Based on CCD photometric observations of 327 stars in *UBV* passbands, we estimated the cluster parameters as, reddening $[E(B-V)] = 1.65 \pm 0.15$ mag and distance $= 2900 \pm 400$ pc. The turn-off age of the cluster was estimated as 25 ± 5 Myr using isochrone fits. *UBV* data of the stars were combined with the *JHK* data from Two-Micron All-Sky Survey (2MASS) and were used to create the near-infrared (NIR) $(J-H)$ versus $(H-K)$ colour–colour diagram. A large fraction of stars (42 per cent) was found to have NIR excess and their location in the diagram was used to identify them as intermediate mass pre-main-sequence (MS) stars. The isochrone fits to pre-MS stars in the optical colour–magnitude diagram showed that the turn-on age of the cluster is 0.3–3 Myr. This indicates that there has been a recent episode of star formation in the vicinity of the cluster.

Slitless spectra were used to identify 27 stars which showed Hα in emission in the field of the cluster, of which six are new identifications. All these stars were found to show NIR excess and are located closer to the region populated by Herbig Ae/Be stars in the $(J-H)$ versus $(H-K)$ diagram. Slit spectra of 25 stars were obtained in the region 3700–9000 Å. The spectral features were found to be very similar to those of Herbig Be stars. These stars were found to be more reddened than the main-sequence stars by 0.4 mag, on an average. Thus, the emission-line stars found in this cluster are more similar to the Herbig Be-type stars where the circumstellar material is the remnant of the accretion disc. We conclude that the second episode of star formation has led to the formation of a large number of Herbig Be stars as well as intermediate mass pre-MS stars in the field of NGC 7419, thus explaining the presence of emission-line stars in this cluster. This could be one of the young open clusters with the largest number of Herbig Be stars.

Key words: stars: emission-line, Be – stars: formation – stars: pre-main-sequence – open clusters and associations: NGC 7419.

1 INTRODUCTION

Young star clusters are formed from molecular clouds, and most of the young clusters can be found along the spiral arms which are known to trigger star formation. A number of young star clusters are located in the Perseus spiral arm in our Galaxy, which are naturally formed and found due to the recent star formation in the spiral arm. Many of the young clusters located here show the presence of a large number of classical Be stars (h & χ Persei, NGC 663, 7419, etc.). In general, these classical Be stars are found to have high rotational velocity resulting in mass loss. This is thought to be the mechanism for the presence of circumstellar material in these stars, which manifests as emission lines (mostly Balmer lines and some Fe lines) in their optical spectra. The overabundance of classical Be stars in a cluster meant that there is some mechanism at work by which a large fraction of the early B-type stars possess high rotational velocity. One of the proposed mechanism is lower metallicity which could increase the stellar rotation. (Maeder, Grabel & Mermilliod 1999). In the case of NGC 146, also located in the Perseus spiral arm with two

⋆E-mail: purni@iiap.res.in

emission-line stars, the cluster was found to have stars as young as 3 Myr, whereas the turn-off age was found to be 10–15 Myr. One of the emission-line stars was identified as Herbig Be star showing signatures of accretion. Subramaniam et al. (2005) thus concluded that the Herbig Be star could have formed from the recent star formation in NGC 146. This opened up another possibility that the clusters in this spiral arm could have experienced continued or episodic star formation resulting in the presence of young stars in the vicinity of the cluster. Since the molecular clouds are abundant in spiral arms, episodic/continuous star formation in the vicinity of already formed clusters is surely possible. Therefore, some of the Be stars found in these clusters could actually be similar to the Herbig Be stars, which are intermediate mass pre-main-sequence (MS) stars.

In order to look into this possibility, it is required to estimate the duration of star formation in a cluster. The duration of star formation is the difference between the turn-off age (estimated from the red giants and the MS turn-off) and the turn-on age (estimated from the pre-MS stars). In some clusters, the difference between the above two ages could be a few Myr, indicating that the star formation was more or less continuous. In the case of NGC 146, the difference was estimated as 7 Myr, which could suggest either episodic or continuous star formation. The age distribution of the identified pre-MS stars can also be used to differentiate between continuous and episodic star formation. In this paper, we study the cluster NGC 7419 in detail to understand the connection between the duration of star formation and the presence of classical Be stars in this cluster.

2 PREVIOUS STUDIES

NGC 7419 is a moderately populated galactic star cluster in Cepheus lying along galactic plane $l = 109.13$, $b = 1.14$ with unusual presence of giants and supergiants (Fawley & Cohen 1974). Blanco et al. (1955) identified the giants/supergiants from objective prism infrared spectroscopy and estimated a visual absorption of 5.0 mag and a distance of 6.6 kpc. van de Hulst, Mullar & Oort (1954) estimated a distance of 3.3 kpc, whereas Moffat & Vogt (1973) estimated the distance to be 6.0 kpc. Photometric observations of the central region of this clusters were made by Bhatt et al. (1993). They found a differential reddening of 1.54–1.88 mag with a mean of 1.71 mag, a cluster distance of 2.0 kpc and age about 40 Myr. Beauchamp, Moffat & Drissen (1994) estimated a younger age of 14 Myr and indicated higher A_V as reported by majority of authors. General absorption is found to be higher in this direction. Pandey & Mahra (1987) and Nickel & Clare (1980) have found an absorption of 2.0–3.0 mag at 2 kpc in this direction. The clusters NGC 7380 ($l = 112\overset{\circ}{.}76$, $b = 0\overset{\circ}{.}46$) and Mark 50 ($l = 111.36$ $b = -0.02$), nearly in the direction of NGC 7419, show a range of mean A_V from 1.8 to 3.4 mag (Leisawitz 1988).

Hα emission stars in NGC 7419 were discovered by Gonzalez & Gonzalez (1956) and Dolidze (1959, 1975). Furthermore, Kohoutek & Wehmeyer (1999) updated this list with more such stars. Pigulski & Kopacki (2000) recently reported that NGC 7419 contains a relatively large number of classical Be stars. From CCD photometry in narrow-band Hα and broad-band R and I (cousin) filters; they identified 31 such stars. The fraction of classical Be stars found in this cluster puts it along with NGC 663, which is the richest in classical Be stars among the open clusters in our Galaxy.

NGC 7419 also contains a low blue–red giants ratio (Beauchamp et al. 1994). Caron et al. (2003) indicated a direct relation between the relative frequency of red supergiants (RSG) stars and classical Be stars. They found that the fraction of RSG increases with rotation, and hence the massive stars may be rapid rotators. Rapid rotation of early-type stars is also used to explain the presence of classical Be stars. NGC 7419 is most likely to have solar metallicity and hence lower metallicity is unlikely to be the reason for fast rotation. The consensus so far, as mentioned by Caron et al. (2003), is that the stars in this cluster were formed from a giant molecular cloud with significantly higher internal motions than what is seen in the surroundings, resulting in the formation of rapidly rotating early-type stars. This suggests that the star formation condition in this region is different from the rest of the regions in the Galaxy, such that the early-type stars end up as rapid rotators, which is very unlikely. They also mention that so far, there is no direct spectroscopic estimation of the metallicity or rotation of stars in this cluster. Hence, the theory of rapid internal motions and different star formation process is not yet verified. Thus the problem of the high fraction of classical Be stars in this cluster is still an open question.

3 OBSERVATIONS

The photometric and the spectroscopic observations of NGC 7419 have been obtained using the Himalayan Faint Object Spectrograph and Camera (HFOSC) available with the 2.0-m Himalayan Chandra Telescope, located at Hanle and operated by the Indian Institute of Astrophysics. Details of the telescope and the instrument are available at the institute's homepage (http://www.iia.res.in/). The CCD used for imaging is a 2 × 4 K CCD, where the central 2 × 2 K pixels were used for imaging. The pixel size is 15 μm with an image scale of 0.297 arcsec pixel^{-1}. The total area observed is approximately 10 × 10 arcmin^2. The log of observations is given in Table 1. The night of the photometric observation was not photometric, therefore we used the previous photometric observations of NGC 7419 (Bhatt et al. 1993) for calibrations. IRAF and DAOPHOT II routines were used to obtain the stellar magnitudes. The error in the zero-point estimations were found to be 0.01 mag in B and V and 0.02 in U passband.

The cluster region was observed in the slitless spectral mode with grism as the dispersing element using the HFOSC in order to identify stars which show Hα in emission. This mode of observation using the HFOSC yields an image where the stars are replaced by their spectra. This is similar to objective prism spectra. The broad-band R filter (7100 Å, bandwidth BW = 2200 Å) and Grism 5 (5200–10 300 Å, low resolution) of HFOSC CCD system was used in combination without any slit. We used the Johnsons R filter in the field to restrict the spectra to the spectral region of the R band. The image is similar to fig. 2 of Subramaniam et al. (2005), which was obtained for NGC 146. Later on, slit spectra of 25 stars identified to show Hα in emission were obtained in the wavelength range, 3700–6800 and 5600–9000 Å using low-resolution grisms 7 and 8. Spectrophotometric standards such as Wolf 1346, BD 284211 and Hiltner 600 were observed on all nights. The spectra of a known Be star, HD 58343 (B3Ve), in the blue region and a known Herbig Be star, HBC 705 (LKHα 147, B2), in the red region were also observed and reduced in a similar way for comparison. All the observed spectra were wavelength calibrated and corrected for instrument sensitivity using IRAF tasks.

The field of the cluster observed photometrically is shown in Fig. 1. The Hα emission-line stars are shown as filled circles among the normal stars (open circles). The pre-MS stars are identified as open circles with crosses within. Our photometry does not have magnitudes for five emission-line stars, and thus the locations of 22 emission-line stars are shown in Fig. 1. These data are used to estimate the cluster parameters as described in the following sections.

Table 1. Log of photometric and spectroscopic observations.

Star/region	Date	Filter/grism	Exposure time (s)
Photometry			
N7419	2004 July 9	V	$3 \times 10, 2 \times 60$
	2004 July 9	B	$30, 60, 2 \times 300$
	2004 July 9	U	$120, 2 \times 600$
Slitless spectra			
Central	2003 October 30	R	5
	2003 October 30	R + grism5	120, 600
	2004 July 9	R	5
	2004 July 9	R + grism5	900
North	2003 October 30	R	5
	2003 October 30	R + grism5	300
South	2003 October 30	R	5
	2003 October 30	R + grism5	120, 600
Slit spectra			
Star	Grism	Exposure time (s)	Date/repeat date
N7419 B	gr7, gr8	900 each	2005 June 27
N7419 D	gr7	900	2005 July 15 (repeat on October 12)
	gr8	1200	2005 July 15
N7419 L, H	gr7	1200	2005 July 15 (repeat on October 8)
	gr8	1200	2005 July 15
N7419 A, I	gr7	1200	2005 July 15 (repeat on October 12)
	gr8	1200	2005 July 15
N7419 C	gr7, gr8	900 each	2005 July 31
N7419 E	gr7	1200	2005 July 31 (repeat on October 9)
	gr8	1200	2005 July 31
N7419 J, G, 3	gr7, gr8	900 each	2005 August 8
N7419 N, O	gr7	900	2005 August 8 (repeat on October 9)
	gr8	900	2005 August 8
N7419 M	gr7, gr8	900 each	2005 August 8
N7419 1, 2, 4, 5	gr7, gr8	900 each	2005 October 7
N7419 6, P, Q, R	gr7, gr8	900 each	2005 October 8
N7419 I1	gr7, gr8	900 each	2005 October 9
N7419 F	gr7, gr8	900 each	2006 January 21
N7419 K	gr7, gr8	900 each	2006 January 21

4 ESTIMATION OF REDDENING, DISTANCE AND AGE

Photometric observations in the *UBV* passbands are used to estimate the reddening and distance to the cluster. There has been indications of differential reddening across the cluster region (Bhatt et al. 1993). The $(U - B)$ versus $(B - V)$ colour–colour diagram of the cluster is shown in Fig. 2. The observed area as shown in Fig. 1 is used to estimate the reddening and all stars within the observed region are used. It can be seen that there is a large variation in reddening within the observed region. The unreddened MS is reddened by two values, $E(B - V) = 1.45$ and 1.85 mag to match the extreme locations of stars in the diagram. The average reddening is found to be $E(B - V) = 1.65 \pm 0.15$ mag. Assuming normal reddening law for the interstellar reddening, the visual extinction towards the cluster is estimated as $3.1 \times 1.65 = 5.1 \pm 0.4$ mag. The reddening and extinction values estimated here are very similar to the previous estimates.

The observed colour–magnitude diagram (CMD) is shown in the left-hand panel of Fig. 3. The narrow MS along with the turn-off and the red giants can be clearly noted. In Fig. 2, it can be noted that there are a few foreground stars which have much less reddening. These stars are likely to cause scatter near the MS turn-off resulting in an inaccurate estimation of the turn-off age. Therefore, stars with $(B - V) \leqslant 1.2$ mag are not considered for age estimation. The reddening and extinction corrected CMD is shown in the right-hand panel of Fig. 3. The zero-age MS (ZAMS) fit to the CMD is used to estimate the distance to the cluster. As shown in the figure, the absolute distance modulus is estimated as 12.3 ± 0.4 mag, which corresponds to a distance of 2900 ± 400 pc. The large uncertainty is due to the differential reddening across the cluster.

The MS turn-off of the cluster along with the red supergiants is used to estimate the post-MS age using the Padova isochrones (Bertelli et al. 1994). In our CMD, we have shown three red supergiants and one bluer giant. This cluster is known to have five red supergiants located close to one another, and found to be members based on radial velocity (Beauchamp et al. 1994). In the right-hand panel of Fig. 3, three isochrones with ages log(age) = 7.3, 7.4 and 7.5 are shown, which correspond to 20, 25 and 32 Myr, respectively. The 25 Myr isochrone is shown as bold line and the other two are shown as dotted lines. The turn-off age of the cluster

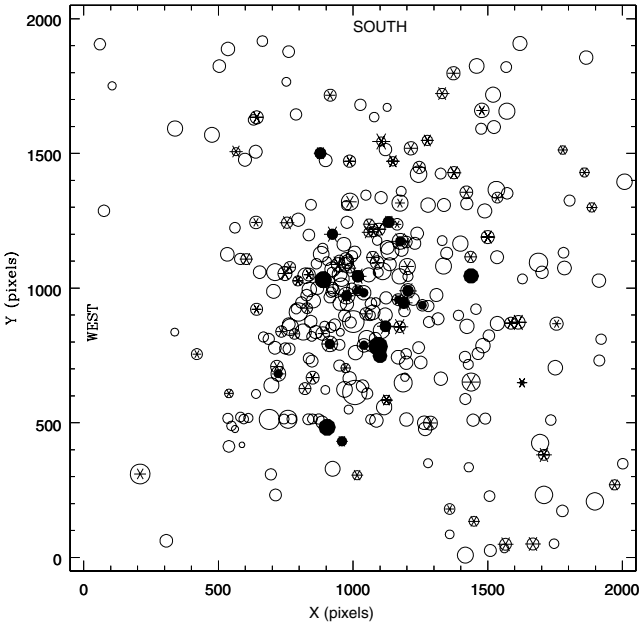

Figure 1. The observed region of the cluster NGC 7419. North is down and east is to the right. Crosses within open circles are stars with NIR excess (pre-MS stars).

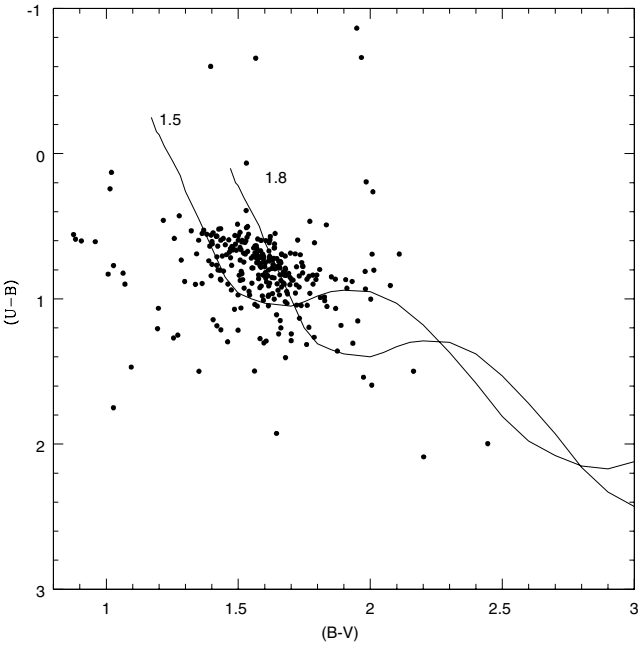

Figure 2. Estimation of reddening towards the cluster using all the stars observed in the cluster region using $(U - B)$ versus $(B - V)$ colour–colour diagram.

is thus found to be between 20 and 30 Myr, while the 25 Myr isochrone visually appears to fit better. Thus, we estimate the age of the cluster as 25 ± 5 Myr. The present age estimate is similar to that derived by Bhatt et al. (1993), but older than that estimated by Beauchamp et al. (1994). We also estimated the age of the cluster using synthetic CMDs. We constrained the number of red supergiants to create synthetic CMDs using PADOVA models (Bressan et al. 1993). The constructed CMDs are similar to those shown in fig. 7 of

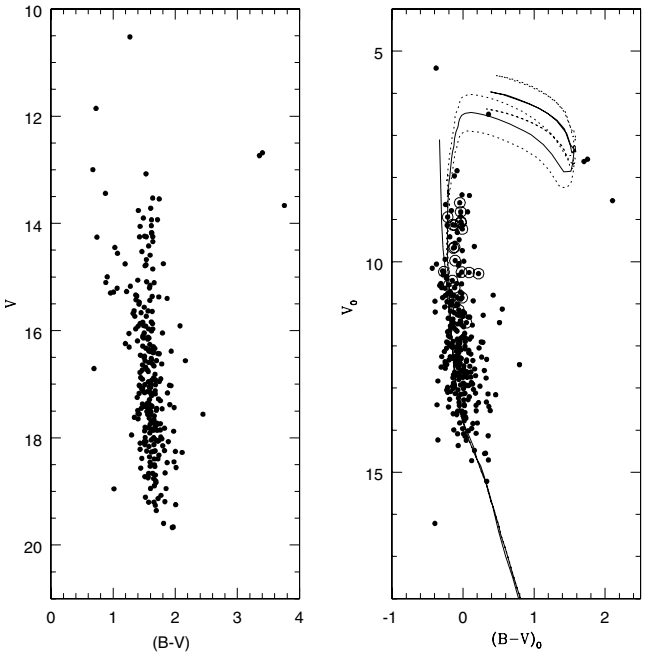

Figure 3. The observed CMD of 327 stars is shown in the left-hand panel. The reddening and extinction corrected CMD after removing the foreground stars is shown in the right-hand panel. Fit of ZAMS and isochrone to the cluster MS and turn-off is also shown. The estimated distance modulus is 12.3 mag. The age of the isochrones shown are 25 Myr (bold line), 20 and 32 Myr (dashed lines). The emission-line stars are denoted by open circles around dots.

Subramaniam et al. (2005). It was found that the best-fitting CMDs were possible for ages 20–22 Myr. For ages younger than 20 Myr, the clump of red giants does not form and also, the tip of the MS is brighter than what is observed. For ages older than 22 Myr, large number of blue supergiants are formed. Therefore, the method of synthetic CMDs estimate the age of the cluster between 20 and 22 Myr, which is similar to the age estimated using the isochrones. Therefore, we confirm that the turn-off age of this cluster is ∼25 Myr. Thus, the cluster is not very young to be populated by intermediate mass pre-MS stars, since these stars typically spend only a few million years in the pre-MS phase. Thus the turn-off age does not indicate any likelihood of the presence of intermediate mass pre-MS stars in the cluster.

5 NEAR-INFRARED DATA AND PRE-MAIN-SEQUENCE STARS

The optical data are cross-correlated with the Two-Micron All-Sky Survey (2MASS) image to identify the common stars in both the data set. Of the 327 stars for which we could obtain *UBV* photometry, we identified near-infrared (NIR) counterparts for 198 stars. Thus, J, H, K magnitudes were combined with the present *UBV* photometry for 198 stars in the cluster region. The $(J - H)$ versus $(H - K)$ colour–colour diagram of all the stars in the cluster region is shown in the left-hand panel of Fig. 4. The diagram also shows the location of MS stars, giants and the reddening line (Bessel & Brett 1988). The two boxes shown are the location where classical Be stars and Herbig Ae/Be stars are generally found (Dougherty et al. 1994; Hernandez et al. 2005). The dashed line indicates the location of T Tauri stars (Meyer et al. 1997). The reddening corrected figure

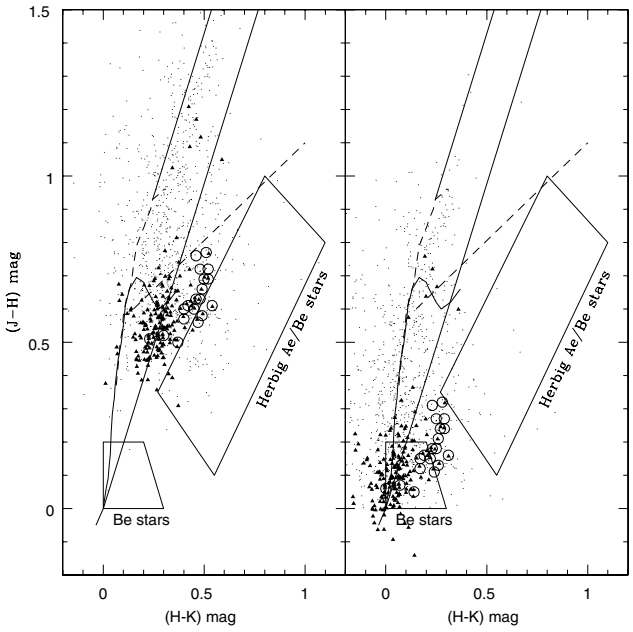

Figure 4. The NIR colour–colour diagram for stars in the region of the cluster is shown in the left-hand panel. The small dots indicate all detections in the observed region, triangles indicate stars with optical counterparts and large open circles indicate emission-line stars. The location of Herbig Ae/Be stars and classical Be stars is also indicated. The location of stars in the diagram after reddening correction is shown in the right-hand panel.

is shown in the right-hand panel. The value of $E(J-H)$ used for reddening correction is 0.45 mag and $E(H-K)$ is 0.23 mag. The black triangles indicate optically identified stars, and the triangles with open circles indicate stars with Hα in emission. The foreground stars are not shown in this figure.

Stars (denoted by triangles) located to the right of the reddening line have NIR excess. It can be seen that the whole cluster sequence is highly reddened with the presence of a large number of stars with NIR excess. 83 stars were found to show NIR excess among the 198 stars. The emission-line stars also show NIR excess, except star K (see Table 2). Due to heavy reddening, the emission-line stars are not found near the Be star box, but are distributed close to the Herbig Ae/Be location and a few of them within the Herbig Ae/Be box. The panel on the right-hand side shows the dereddened sequence. Some of the stars show negative colour due to over correction of the reddening, due to variable reddening in the region. It can be seen that some emission-line stars are now located in the Be box, though a large fraction still lies outside. The stars are in fact located in a region which connects the loci of classical and Herbig Be stars, with a couple of emission-line stars located within the Herbig Ae/Be box. It is necessary to find the evolutionary status of these stars in order to understand their peculiar location in the diagram. It can also be seen that the stars with NIR excess are located below the dashed line (just above the location of Herbig Ae/Be stars), which denotes the location of T Tauri stars. Thus, the optically identified stars with NIR excess are most likely to be intermediate mass pre-MS stars. If we extend this argument to the emission-line stars, then it is likely that these stars could also belong to the same category. We find that

Table 2. Photometric data of the identified emission-line stars are tabulated. The first column represents the identification used here, and the second column represents their number in Beauchamp et al. (1994). Columns 3–7 are our data, Columns 8–9 are taken from Pigulski & Kopacki (2000). Columns 10–12 are from 2MASS catalogue, and the reddening in the last column is derived from their blue spectra. The error in the estimated reddening is 0.1–0.2 mag.

Our number	BMD	X (pixel)	Y (pixel)	V (mag)	$(B-V)$ (mag)	$(U-B)$ (mag)	Rc (mag)	$(R-I)$c (mag)	J (mag)	H (mag)	K (mag)	$E(B-V)$ (mag)
A	1076	1438.18	1045.17	14.34	1.64	0.55	13.21	1.15	10.41	9.81	9.36	2.2
B	831	1203.74	989.98	14.77	1.53	0.51	13.78	1.03	11.41	10.80	10.26	1.9
C	781	1167.58	957.21	14.06	1.43	0.52	12.89	1.09	9.90	9.27	8.79	2.0
D	728	1120.37	858.29	15.56	1.50	0.57	14.78	1.01	12.22	11.66	11.19	2.1
E	745	1132.46	1245.57	16.56	1.70	0.69	15.39	1.18	12.44	11.75	11.25	2.0
F	741						16.08	1.21	13.09	12.37	11.89	2.3
G	620	1040.42	787.60	14.25	1.54	0.54	13.12	1.14	10.36	9.70	9.21	1.9
H	582	1017.98	1044.08	15.67	1.45	0.63	14.63	1.02	11.61	11.04	10.64	2.1
I	585	1017.98	1044.08	14.24	1.51	0.54	13.44	1.02	11.03	10.53	10.16	2.1
I1	OUT											2.4
J	417	913.54	792.92	13.93	1.62	0.61	13.14	1.06	10.46	9.94	9.64	2.0
K	621	1039.66	989.00	14.79	1.51	0.61	13.93	1.12	11.33	10.82	10.59	2.3
L	504	975.81	971.92	15.09	1.54	0.55	14.08	1.11	11.43	10.85	10.36	2.2
M	389	889.31	1031.15	13.72	1.60	0.60	12.64	1.14	9.95	9.32	8.84	2.1
N	427	923.62	1200.29	15.37	1.74	0.70	14.03	1.23	10.98	10.29	9.77	2.2
O	232						15.51	1.33	12.12	11.35	10.84	2.2
P	OUT	878.74	1500.79	15.36	1.63	0.73			11.50	10.89	10.47	2.1
Q	OUT	903.56	483.38	15.97	1.64	0.62			12.18	11.55	11.09	2.2
R	OUT	959.03	431.47	16.09	1.48	0.65			12.49	11.89	11.49	2.2
S	OUT								12.07	11.31	10.85	–
T	OUT								12.93	12.21	11.69	–
1	884	1257.71	936.35	15.73	1.53	0.58	14.64	1.07				2.1
2	815	1188.64	945.16	15.35	1.38	0.55	14.58	1.02				2.2
3	692	1093.24	783.30	14.19	1.62	0.57	13.05	1.15				1.8
4	702	1100.23	748.24	14.17	1.62	0.59	13.15	1.13				2.1
5	239	722.58	682.02	15.40	1.87	0.86	13.90	1.31				2.3
6	795	1174.97	1173.92	16.26	1.59	0.72	15.02	1.17				2.1

the fraction of pre-MS stars is 42 per cent, which is almost half of the stars in this cluster. These pre-MS stars are very likely to be very young and their age is estimated in the following section.

6 PRE-MAIN-SEQUENCE AGE ESTIMATION

In general, the right side of the MS at the fainter end of the cluster CMD is populated with field giants. But this is the same region which is occupied by the pre-MS stars, if they are present in the cluster. In the previous section, we identified some stars to have NIR excess which have optical counterparts. If these are pre-MS stars, then they should be located to the right of the MS in the optical CMD. In other words, the presence of NIR excess and their location in the NIR colour–colour diagram can be used to identify the pre-MS stars from the field stars in the right side of the CMD. The cluster CMD is shown in Fig. 5, where only stars with NIR excess are shown, and the emission-line stars are shown as dots with circles around them. It can be seen that most of these stars are located to the right side of the MS. This confirms that the stars with NIR excess are pre-MS stars. Also, a large fraction (42 per cent) of stars are in the pre-MS phase. In order to estimate the age of these pre-MS stars, pre-MS isochrones from Siess, Dufour & Forestini (2000) are plotted on the figure. The isochrones shown are for ages 0.2, 0.3, 0.4, 0.5, 1.0, 1.5, 3.0, 5.0 and 10 Myr in dashed lines. The post-MS isochrone of age 25 Myr and ZAMS are also shown as continuous lines. Emission-line stars, which have $V_0 \sim 10.0$ mag and fainter, are well matched by the isochrones of ages 0.3–1.0 Myr. It can be seen that the clump of emission-line stars located at $(B - V)_0 \sim 0.0$ mag and $V_0 \sim 11.0$ mag is located just brighter than the 0.3 Myr pre-MS isochrone, and the isochrones do not reach this location. One possible reason is that these stars are more massive than 7.0 $M_\odot$, which is the upper mass limit of the model used. These stars could also be younger than 0.3 Myr. Therefore, all the emission-line stars are found to have ages less than 1.0 Myr. A number of stars with NIR, which did not show any Hα emission, are found to have ages between 0.5 and 3.0 Myr. Only two stars are found to be older than 3.0 Myr. The limiting magnitude of the CMD is $V_0 \sim 15.0$ mag, and only two stars are found in the magnitude range of 13.0–15.0 mag. Thus, it is very likely that there are very few pre-MS stars with ages older than 3.0 Myr. Thus, the 42 per cent of the stars in the cluster are likely to have formed in the last 3 Myr or less than that.

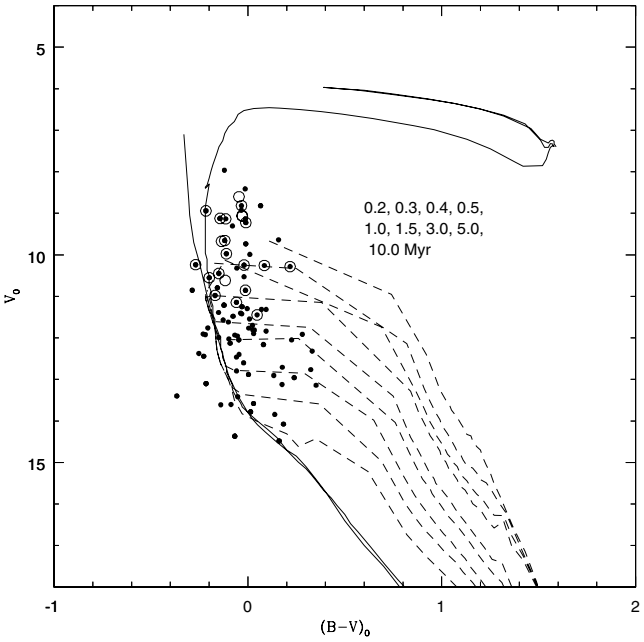

Figure 5. The optical CMD of stars with NIR excess. The dots with circles around them are the emission-line stars. The pre-MS isochrones of Siess et al. (2000) for various ages are shown in dashed lines. The post-MS isochrone of age 25 Myr and ZAMS is shown in continuous lines.

Since we have estimated the turn-off and the turn-on age, we will now discuss the *star formation history* of the cluster. The values derived for the age of the cluster from the turn-off and the turn-on are quite different, since the post-MS age of the cluster is found to be much higher than the pre-MS age (25 and 3 Myr). It is very unlikely that the pre-MS and the turn-off stars belong to the same population, as the star formation in the cluster is unlikely to have continued for more than 20 Myr. It is more likely to come from two different bursts of star forming events. The presence of the pre-MS stars can be understood if the cluster has experienced a recent event of star formation in its vicinity. This star formation is likely to have happened in the last 3 Myr with most of the massive stars forming in the last 0.3 Myr. Thus, we propose that NGC 7419 cluster region experienced two episodes of star formation, one around 25 Myr and the second between 0.3 and 3 Myr. The pre-MS isochrone fits clearly point out that at least 12 stars with Hα emission have age as young as 0.3 Myr. The brighter emission-line stars are also likely to belong to this group. In the optical CMD, all the emission-line stars are more reddened than the MS. Also, in the NIR colour–colour diagram, they are not located in the location for Be stars, but in a region with larger reddening and NIR excess and thus closer to the location of Herbig Ae/Be stars. Combining all the above, it is very clear that the so-called classical Be stars in this cluster are more likely to be very young pre-MS stars in the B-spectral type. Thus, these stars are similar to the Herbig Be stars in their evolutionary state and not to the fast rotating classical Be stars. In the following section, we present the spectra of the emission-line stars and compare them with the spectra of classical and Herbig Be stars.

7 EMISSION-LINE STARS

Pigulski & Kopacki (2000) found 31 Be stars in the central region of the cluster using Hα photometric observations. In order to confirm their identification, we obtained slitless spectra of the central as well as the northern and southern regions. The spectra of stars brighter than $V = 16.0$ mag could be identified by this technique. This technique helps to identify stars with medium to strong Hα emission. When there is a fill up of the absorption line due to emission, this technique fails to identify such stars. Also, near the centre of the cluster, due to crowding effects, spectrum from a fainter star gets submerged within that of a brighter star. Thus, this technique picks up genuine and bona fide Hα emission stars and could result in incomplete detection of the emission-line stars due to the above mentioned problems. Slitless spectra were obtained on two to three epochs in order to identify emission stars which could have been missed out due to variable Hα emission. After analysing these images, we could detect 21 emission-line stars in the same region as studied by Pigulski & Kopacki (2000), against their detection of 31 stars. Outside the central region, we detected six more stars, thus increasing the total number of detections to 27. We do not detect emission in 10 stars which are previously found to show emission. Of these, four stars were found to be too faint to detect their spectrum, four stars were found to show continuum spectrum without any lines and two stars were found to show Hα in absorption. Photometric information of the 27 emission stars is tabulated in Table 2.

R and $(R - I)$ colour are taken from Pigulski & Kopacki (2000). Reddening to individual stars is estimated from their spectra.

The location of the emission-line stars in the optical CMD indicates that they are brighter than $M_V = -2.0$ mag; thus these stars are early B-type stars. We have obtained *UBV* photometry of 22 emission-line stars, which are shown in Fig. 1. We do not have the *UBV* photometric data for stars F, I1 and P due to high photometric errors and stars S and T are out of the field of photometric observation. 2MASS J, H, K data either are not available or have high errors for stars 1–6. In order to understand the nature of these emission-line stars, we obtained slit spectra in the range 3800–9000 Å for 25 emission-line stars. The blue part of the spectrum is shown in Figs 6–8. For comparison, we have also shown the spectrum of a Herbig Be star HBC 705 (spectral type B3, shown in red), which is taken from Hernandez et al. (2004). It can be seen that the spectral features and the slope of the continuum are very similar. Also shown is the spectrum of HD 58343, a known Be star of spectral type B3 and having $V_{\rm rot} < 40$ km s^{-1} (Slettebak et al. 1992). This is shown in blue colour in the figures.

The striking feature of the spectra of emission-line stars is its slope. Just the slope of these B-type stars suggests that they belong to the late type, in sharp contrast to the spectrum of the classical Be star, HD 58343. A comparison with the spectrum of HBC 705 reveals that it could be of a B-type star with very high extinction. Thus, the spectra in the blue region of the emission-line stars indicate that all have high extinction.

The prominent lines in the spectrum are indicated. The presence of 4026, 4121 and 4388 Å He I absorption lines in the spectra indicates that these stars are indeed early-type B stars. This supports the photometric spectral type derived based on the estimated distance. There are a number of features present in the spectra, which are similar to that in the spectrum of the Herbig Be star. This striking similarity of the spectra with that of Herbig Be spectra than that of a Be star spectrum supports the earlier result that these stars are very young pre-MS stars. The width of the Hγ line is similar to

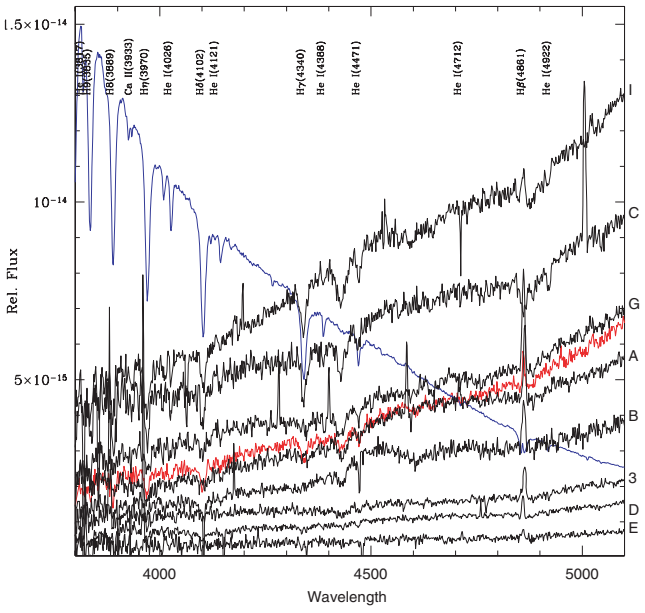

Figure 6. Low-resolution spectra of stars A, B, C, D, E, G, I and 3. Prominent spectral lines are also shown. For comparison, the spectra of HBC 705, a B2 Herbig Be star (red) and HD 58343, a B3Ve, classical emission-line star (blue) are also plotted.

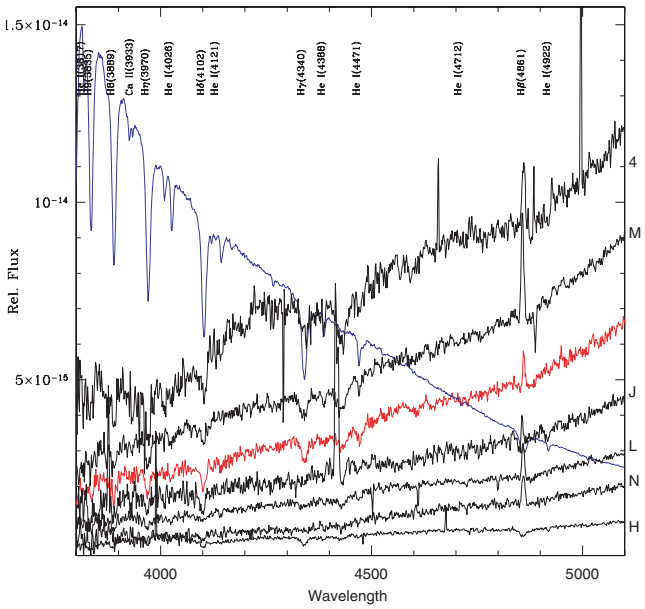

Figure 7. Same as Fig. 6, but for stars, H, J, L, N, M and 4.

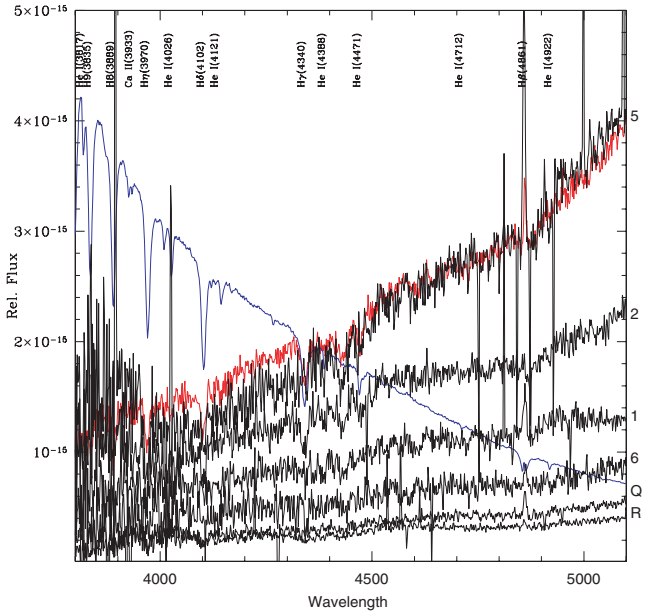

Figure 8. Same as Fig. 6, but for stars Q, R, 1, 2, 5 and 6.

that of the Be star, indicating that the rotation velocity is similar. In some stars, this line is found to show structures indicating that there could be some fill up in the absorption. The Hβ line is found to be in emission in most of the stars. This part of the spectrum is used to estimate the reddening towards each star by dereddening the spectra. The comparison spectrum used is a B3 star spectrum from the spectral library. These reddening estimates are shown in Table 2. The error in the estimate is 0.1 mag for brighter stars and 0.2 for fainter stars where the spectra are noisy. On an average, the emission-line stars have reddening of 2.1 mag, which is ∼0.4 mag more than that estimated for the MS stars. This indicates that the emission-line stars have circumstellar material with a visual

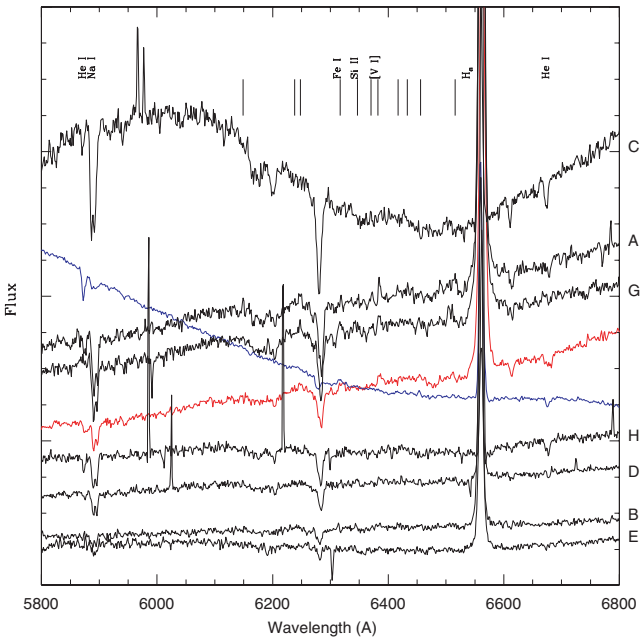

Figure 9. Low-resolution spectra in Hα region. The spectra are labelled. The red and blue spectra indicate HBC 705 and HD 58343, respectively.

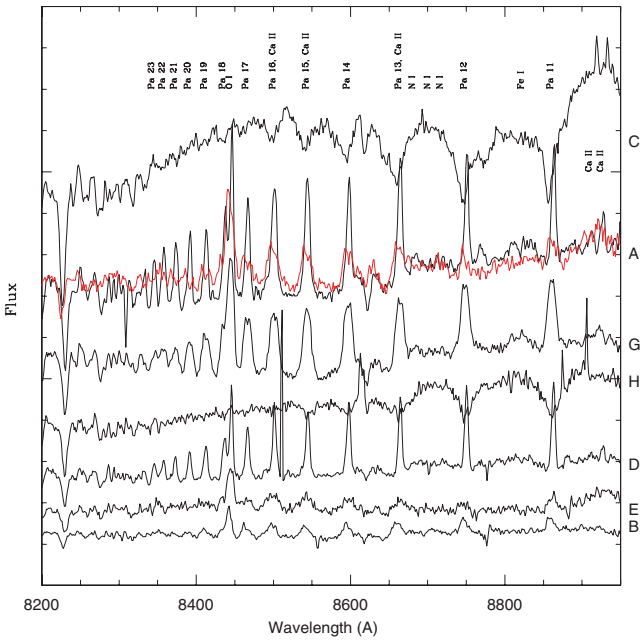

Figure 10. Low-resolution spectra of emission-line stars near the red region. The spectra are labelled and prominent lines are listed. The spectrum of HBC 705 is shown in red for comparison.

extinction of ∼1.2 mag. The spectra of stars F, I1, K, O and P are not shown since the spectra are very noisy.

Spectra of some stars in the region 5800–6800 Å are shown in Fig. 9. Strong Hα emission can be noted in all the spectra. A number of Fe II lines can be seen in emission and these are indicated in the figure. The Hα emission line does not show prominent wings, and the structure is very similar to that seen in HBC 705 (spectrum shown in red colour). In this part of the spectrum also, the spectra show remarkable similarity to that of the Herbig Be star. The He I (6678 Å) is seen in absorption, but shows structures in the profile in some stars, indicating that there is emission within the absorption. This feature is also seen in the spectrum of HBC 705.

The red spectra of these stars indicate the presence of a few more Fe emission lines. O I (7773 Å) is found to be in emission in most of the stars. The red spectrum in the region of Ca II triplet and Paschen lines is shown in Figs 10 and 11. The spectrum of HBC 705, obtained using the Himalayan Chandra Telescope (HCT) is over plotted in red. Various spectral lines are indicated in the figure. In most of the stars, O I (8446 Å) and the Paschen lines are in emission. The presence of Ca II triplet cannot be identified since they get merged with the emission lines of the Paschen series. In the case of star I, the spectrum shows faint Paschen emission lines, whereas the emission lines near the Ca II triplet is stronger which may indicate a significant contribution from Ca II triplet. These emission profiles are found to show structures. Also the Paschen emission lines in 12 stars (C, G, E, B, I, N, L, 3, 4, 2, 1 and Q) are found to show structures, like in the spectrum of HBC 705. In stars, 5, M, J, O, A and D, single peaked strong emission could be seen. The emission profiles indicate the presence of disc around the star. Multiple emission peaks indicate velocity structure/gradient in the disc. Since these emission-line stars belong to the early B type, the presence of low-ionization lines indicates that either these stars have a large amount of circumstellar material or the disc is quite extended. Since the emission profiles are quite sharp, large velocity gradient in the disc is unlikely to be present. Estimation of large circumstellar reddening (0.2–0.6 mag) supports the suggestion that these stars have a large

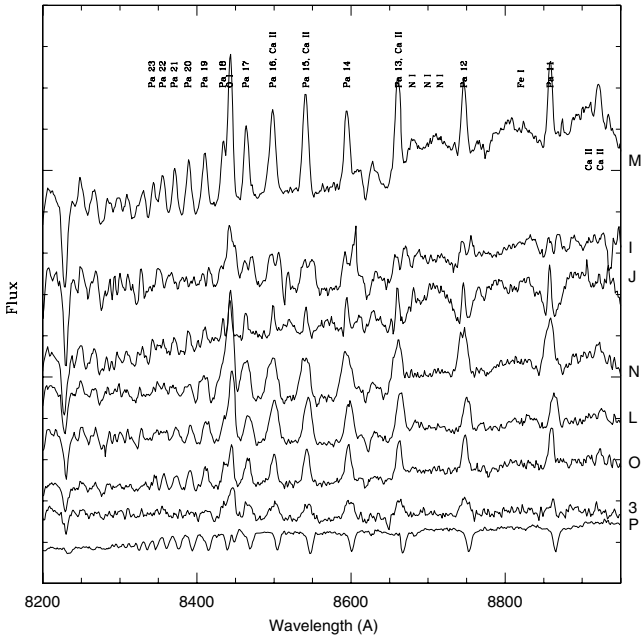

Figure 11. Same as Fig. 10, without the spectrum of HBC 705.

amount of material around them. This again indicates that these stars are similar to the Herbig Be-type stars than the classical Be stars. The stars F and I1 show no absorption or emission features, whereas H, K, P, R and 6 show a few absorption features in this region of the spectrum. Caron et al. (2003) presented high-resolution spectra of M (389), J (417) and G (620) in the region 8300–8900 Å. They also find strong emission in Paschen lines in the spectra of M and G, with a lot of structure in the emission lines of G. We see only a marginal evidence of structure in our spectrum of star G, but it is seen very clearly in the high-resolution spectrum of

Caron et al. (2003). The star J (417) displays weak emission, similar to a shell, in both the low-resolution and high-resolution spectra. Thus, the features identified here are in complete agreement with high-resolution spectra in the red region presented in Caron et al. (2003).

From the spectra presented here, it is clear that the emission stars in this cluster have features very similar to those found in a Herbig Be star than in a classical Be star. Also, the spectra indicate the presence of circumstellar disc and high extinction. No indication of high rotational velocity, either in the stellar absorption lines or in the circumstellar emission lines is seen. This result, in combination with the presence of NIR excess, high circumstellar reddening and a very young pre-MS age, strongly suggests that these stars are Herbig Be-type stars. Thus, the circumstellar disc is the remnant of the accretion disc of the pre-MS phase and is not formed due to fast rotation.

8 COMPONENTS OF REDDENING TOWARDS THE CLUSTER

The reddening estimated towards the normal and the emission-line stars can arise due to a number of components located in the line-of-sight. In the case of this cluster, we were able to deconvolve the various components. The cluster can be reddened due to (i) *interstellar* material located between the cluster and us, (ii) the *circumcluster* material which is left behind after the star formation event and (iii) the *circumstellar* material around the pre-MS stars. We estimate the three components mentioned above. The clusters NGC 7510 ($l = 110\overset{\circ}{.}90$ and $b = 0\overset{\circ}{.}06$) and King 10 ($l = 108\overset{\circ}{.}48$ and $b = -0\overset{\circ}{.}40$) are young clusters (30 and 25 Myr, respectively) located in same direction of NGC 7419. They also have similar distance moduli (12.5 and 12.6), but are located marginally farther away. The estimated value of reddening towards these clusters is $E(B - V) = 1.0$ mag. Thus, the reddening to similarly aged clusters located at similar distance in the same direction is less by 0.65 mag. NGC 7226 is another cluster located in the same direction but slightly older, 300 Myr. This cluster is located at 2 kpc, and the estimated reddening towards this cluster is 0.5 mag. NGC 7245, located at 2 kpc in the same direction, is also found to have a reddening of 0.5 mag. Thus it can be seen that in this direction, the reddening increased between 2 and 3 kpc by 0.5 mag, whereas up to 2 kpc it is only 0.5 mag. Thus we estimate that the reddening due to the component (i) is 1.0 ± 0.15 mag. The estimated reddening to NGC 7419 is 1.65 mag, which is higher than that found for this distance. The fact that the cluster stars are more reddened indicates that some material is present in the immediate vicinity of the cluster. Thus the reddening due to the circumcluster material is 0.65 ± 0.15 mag. Thus we find that there is substantial reddening just around the cluster and this supports the result that the cluster region experienced a recent episode of star formation. Thus the estimate for the second component of reddening (ii) is 0.65 ± 0.15 mag. Now the emission-line stars are found to have NIR excess and higher reddening. We estimated the third component (iii) for these stars using their spectra. The average value of the circumstellar reddening for the emission-line stars is found to be 0.4 ± 0.1 mag, as estimated in the previous section. To summarize, the reddening decomposition shows that there is significant *circumcluster* material, supporting the idea of a recent star formation event in the cluster region. The emission-line stars are thus more likely to be formed as a result of this star formation event and are early-type pre-MS stars, with substantial circumstellar reddening.

9 *XMM* OBSERVATIONS

Early B-type stars can show Hα in emission, if they are in accreting binary systems. There was a proposal by Christian Motch to detect X-ray emission from the emission-line stars in this cluster and NGC 663. The proposal was to search for Be plus white dwarf binaries in a sample of Be-rich young open clusters. These two clusters are found to have a large fraction of Be stars among the B stars, and it was suspected that many may be accreting binary systems. *XMM* has the capability to efficiently detect white dwarfs accreting from the circumstellar envelopes of Be stars. This cluster was observed by *XMM* on 2004 February 2 and the data became public on 2005 April 16. There are 63 sources detected in the direction of NGC 7419. By comparing with the optical data, we find that none of these detections coincides with the Be stars. A few optically faint sources are found to be detected in X-ray and these may be low-mass pre-MS stars like T Tauri stars. A number of sources have also been detected outside the radius of this cluster. Thus, we conclude that the X-ray flux from these stars are below the detection limit of *XMM* observations. Since these observations were expected to detect X-ray binaries at this distance, the non-detection shows that none of these Be stars is accreting binaries.

10 RESULTS AND DISCUSSION

The optical and NIR photometry of stars in the region of the young cluster NGC 7419 is used to estimate the cluster parameters. The estimated values of reddening and distance towards the cluster, and the turn-off age are found to be similar to the previous estimates. By combining the optical and NIR photometry, we identified the presence of a large number of stars (83 stars, 42 per cent) with NIR excess. These stars were found to be intermediate mass pre-MS stars in accordance with their location in the NIR colour–colour diagram and optical CMD. The age of these pre-MS stars is found to be between 0.3 and 3 Myr, whereas the age of the cluster as obtained from the turn-off is found to be 25 ± 5 Myr. These two ages are possible for the same cluster, if the cluster region experienced two episodes of star formation, one at 25 Myr and the other at about 3 Myr. We find that 42 per cent of stars in this region could belong to the recent star formation episode. The slitless spectra of the cluster region revealed the presence of 27 emission-line stars, where six are new detections. All the emission-line stars (except one) have NIR excess and are found to have ages less the 1 Myr, with some as young as 0.3 Myr. Analysis of the slit spectra of 25 stars showed that the spectra closely resemble a Herbig Be star spectrum than a classical Be star spectrum. The spectra show evidence for the presence of circumstellar disc and a large amount of circumstellar material. The reddening estimated from the spectra showed that the emission-line stars are more reddened by 0.4 mag than the normal cluster stars. Thus, we conclude that the emission-line stars found in this cluster are more likely to be Herbig Be-type stars, which are the early-type pre-MS stars and not classical Be stars. Also, *XMM* observations showed that the Be stars in this cluster are not likely to be accreting binary systems. The cluster is also found to have circumcluster reddening of 0.65 mag supporting the evidence for a recent star formation event in the cluster region. By definition, Herbig Be stars are those which have nebulosity around them. In this case, we could not detect any nebulosity, maybe because the cluster is located at large distance.

As shown in Fig. 1, the pre-MS stars are found to be located uniformly across the cluster. On the other hand, the Be stars are found to be located closer to the cluster centre. This might indicate

that the more massive stars are formed preferably towards the cluster centre. We are unable to quantify this statement since stars formed in two episodes cannot be separated. In this cluster, we find that the second episode of star formation has occurred between 0.3 and 3 Myr. Since the upper age limit of the emission-line stars is 1 Myr, we can conclude that the accretion disc for the early B-type stars can survive at least up to 1 Myr. This cluster is most probably the only known open cluster with the largest number of Herbig Be stars. This cluster thus gives a rare opportunity to understand the accretion disc around intermediate mass pre-MS stars as a function of their mass. It is likely that there are high mass ($\geqslant 7\,M_{\odot}$) stars in the pre-MS phase, which are also as young as 0.3 Myr. Therefore, this cluster is very ideal to test the pre-MS evolutionary models of stars in this mass range.

The presence of a large number of classical Be stars among the early-type B stars in this cluster has been a puzzle. In this paper, we argue that the emission-line stars present in this cluster are not classical Be stars, but Herbig Be stars. In the earlier sections, we found that the cluster requires some special property like lower metallicity or chaotic cloud environment to explain a large fraction of Be stars. In the present scenario, no such special property is required for the cluster or the environment. Since the cluster is located in the Perseus spiral arm, multiple star formation episodes are possible in the vicinity of the cluster. The implication of the present result is that in young open clusters, the emission-line stars may not have been identified properly. There could be genuine classical Be stars, but there is also the possibility that they are not fast rotators, but those with the remnant of the accretion disc. In this cluster, we find that the emission-line stars populate the region between the location for classical and Herbig Be stars in the NIR colour–colour diagram. The spread in their distribution in the figure is most likely due to the difference in the amount of circumstellar material around them. The distribution of their location in the diagram points to the possibility that with the evaporation of the disc, these stars can gradually come down along the reddening vector, to populate the region of classical Be stars. If this is the case, then can some of the stars located in the classical Be region be evolved Herbig Be stars? In short, can the Herbig Be stars evolve to become a classical Be star without fast rotation? If possible, then what is the time-scale required? We plan to study more open clusters with classical Be stars in order to address this question.

This study has demonstrated that it is very important to combine the optical and NIR data for young open clusters to understand the properties of the cluster. The NIR data in combination with the optical data can be effectively used as a tool to differentiate pre-MS stars from the field stars. It is also very essential to derive not only the turn-off age, but also the turn-on age using the pre-MS stars. These two ages are required to identify the presence of any continued/episodic star formation in the vicinity of the cluster. We also find that continued/episodic star formation around clusters located on spiral arms is not uncommon. Another point to look into is the effect of episodic/continued star formation from the context of initial mass function. When the initial mass function of a cluster is estimated, one generally assumes that the cluster is formed in one single burst of star formation and that all the stars have almost the same age. We find that this assumption need not be correct (e.g. NGC 146) and in some cases, like NGC 7419, it can be completely wrong. Continued or episodic star formation in the cluster region can lead to the presence of pre-MS stars and thereby to an inaccurate estimation of the mass function slope. Therefore, understanding the *star formation history* of young clusters is necessary before one attempts to estimate various cluster parameters.

ACKNOWLEDGMENTS

We thank the staff of Indian Astronomical Observatory, Hanle and at CREST campus, Hosakote for assistance during observations. This research has made use of WEBDA database, operated at the Institute for Astrophysics, University of Vienna. This publication makes use of data products from the Two Micron All Sky Survey, which is a joint project of the University of Massachusetts and the Infrared Processing and Analysis Center/California Institute of Technology, funded by the National Aeronautics and Space Administration and the National Science Foundation.

REFERENCES

Beauchamp. A., Moffat A. F. J., Drissen L., 1994, ApJS, 93, 187
Bertelli G., Bressan A., Chiosi C., Fagotto F., Nasi E., 1994, A&AS, 106, 275
Bessel M. S., Brett J. M., 1988, PASP, 100, 1134
Bhatt B. C., Pandey A. K., Mohan V., Mahra H. S., Paliwal D. C., 1993, BASI, 21, 33
Blanco V., Nassau J. J., Stock J., Wehlau E., 1955, ApJ, 121, 637
Bressan A., Fagotto F., Bertelli G., Chiosi C., 1993, A&AS, 100, 647
Caron G., Moffat A. F. J., St-Louis N., Wade G. A., 2003, AJ, 126, 1415
Dolidze M. V., 1959, Bull. Abastumani Astron. Obs., 24, 7
Dolidze M. V., 1975, Bull. Abastumani Astron. Obs., 47, 3
Dougherty S. M., Waters L. B. F. M., Burki G., Cote J., Cramer N., van Kerkwijk M. H., Taylor A. R., 1994, A&A, 290, 609
Fawley W. M., Cohen M., 1974, ApJ, 193, 367
Gonzalez G., Gonzalez G., 1956, Boletin de los Observatorios Tonantzintla Tacubaya, 15, 16
Hernandez J., Calvet N., Briceno C., Hartmann L., Berlind P., 2004, AJ, 127, 1682
Hernandez J., Calvet N., Hartmann L., Briceno C., Sicilia-Aguilar A., Berlind P., 2005, AJ, 129, 856
Kohoutek L., Wehmeyer R., 1999, A&AS, 134, 255
Leisawitz D., 1988, Catalogue of Open clusters and Associatied Interstellar Matter, NASA Reference Publication
Maeder A., Grabel E. K., Mermilliod J.-C., 1999, A&A, 346, 459
Meyer M. R., Beckwith S. V. W., Herbst T. M., Robberto M., 1997, ApJ, 489, 173
Moffat A. F. J., Vogt N., 1973, A&A, 23, 317
Nickel Th., Clare G., 1980, A&AS, 42, 251
Palla F., Stahler S. W., 1993, ApJ, 418, 414
Pandey A. K., Mahra H. S., 1987, MNRAS, 226, 635
Pigulski A., Kopacki G., 2000, A&AS, 146, 465
Siess L., Dufour E., Forestini M., 2000, A&A, 358, 593
Slettebak A., Collins G. W., Truax R., 1992, ApJS, 81, 335
Subramaniam A., Sahu D. K., Sagar R., Vijitha P., 2005, A&A, 440, 511
van de Hulst H. C., Mullar C. A., Oort J., 1954, BAN, 12, 117

This paper has been typeset from a TEX/LATEX file prepared by the author.